This article has been accepted for publication in IEEE Transactions on Biomedical Engineering. This is the author's version which has not been fully edited and content may change prior to final publication. Citation information: DOI 10.1109/TBME.2025.3607144

Sudden Cardiac Death Risk Prediction from QT–RR Adaptation Time Lag Computed from Exercise Stress Test ECG

Cristina Pérez, Juan Pablo Martínez, Julia Ramírez, Tuomas Kenttä, Juhani Junttila, Antti Kiviniemi, Juha Perkiömäki, Heikki Huikuri, Esther Pueyo, and Pablo Laguna, *Fellow, IEEE*

***Abstract*— *Objetive:* This study aims to evaluate the QT adaptation time following gradual heart rate changes estimated from exercise stress test (EST) ECGs as a marker of sudden cardiac death (SCD) risk. The predicted risk value for any cardiovascular death (CVD) is also evaluated.**

***Methods:* Three ECG-derived markers related to QT-RR adaptation time were estimated during the exercise phase of EST, τ_e, during the recovery phase, τ_r, and as the difference between them, Δ_τ. The values were computed from patients with coronary artery disease (CAD) from ARTEMIS study (N=1472; median follow-up of 8.9 years). These markers are calculated as the delay between the observed RR interval series and a patient-specific memoryless RR series computed from the QT interval (RR-based strategy). Alternatively, the estimates were calculated as the delay between the observed QT intervals and a patient-specific instantaneous QT series computed from the RR intervals (QT-based strategy). The relation between the markers and CAD or SCD was evaluated.**

***Results:* The marker τ_r is more robustly estimateed with the RR-based strategy and is able to stratify survivors and victims of either SCD or CVD (p-value equal to 0.022 and 0.065, respectively). Multivariable regression models for predicting SCD and CVD include the QT-RR adaptation time estimated in the recovery phase of EST using the RR-based strategy.**

***Conclusion*: A prolonged QT-RR adaptation time during the recovery phase of the EST ECG, calculated with the RR-based strategy, can predict SCD and CVD, providing complementary information to other clinical markers.**

***Index Terms*— QT-RR modeling, QT-RR adaptation time lag, exercise stress test, sudden cardiac death.**

Manuscript submitted on August 6, 2025. The work was supported by projects PID2021-128972OA-I00, PID2022-140556OB-I00, PID2023-148975OB-I00, CNS2023-143599, and TED2021-130459B-I00 funded by Spanish Ministry of Science and Innovation (MICINN) and FEDER, by Gobierno de Aragón (Reference Group Biomedical Signal Interpretation and Computational Simulation (BSICoS) T39_23R and project LMP94_21). JR acknowledges funding from the European Union-NextGenerationEU, fellowship RYC2021-031413-I from MCIN/AEI/10.13039/501100011033, and from the European Union "NextGenerationEU/PRTR". The computation was performed at the High Performance computing platform of the NANBIOSIS ICTS *(Corresponding author: Cristina Pérez)*.

C. Pérez, E. Pueyo, J.P. Martínez, J. Ramírez and P. Laguna are with the Biomedical Signal Interpretation & Computational Simulation Group (BSICoS), Aragón Institute of Engineering Research (I3A), Zaragoza University, Zaragoza, IIS Aragón and CIBER-BBN, Spain (cperez@unizar.es). Tuomas Kenttä, Juhani Junttila, Juha Perkiömäki, Antti Kiviniemi, and Heikki Huikuri are with Research Unit of Internal Medicine, Medical Research Center Oulu, University of Oulu and Oulu University Hospital, Oulu, Finland.

I. Introduction

CORONARY artery disease (CAD) is the most common underlying substrate of sudden cardiac death (SCD), often due to ventricular arrhythmias (VAs), which progress from ventricular tachycardia to ventricular fibrillation [1]. Ventricular fibrillation is characterized by uncoordinated electrical impulses due to division of the cardiac impulse along multiple pathways, leading to rapid and ineffective ventricular contractions. Enhanced ventricular repolarization heterogeneity can contribute to an increased risk of VAs and SCD [2], [3]. Today, SCD remains a major public health problem and accounts for 15-20% deaths in Western societies [4].

The 2022 European Society of Cardiology guidelines indicate that a multifaceted approach that incorporates cardiac magnetic resonance imaging, genetic testing, and clinical history is required in the management of VAs and the prevention of SCD by guiding the implantation of cardioverter defibrillators (ICDs) [5]. Moreover, the importance of ECG analysis is recognized, even if many previously proposed ECG markers are still not included in existing risk calculators [6]. This is because the ECG remains the most commonly used cardiovascular diagnostic tool due to its wide availability, low cost and rapid interpretation [7]–[9].

The most established ECG marker for arrhythmic risk prediction is the QT interval [10]. This interval presents a strong dependence on heart rate and is usually corrected for its effects [10]–[12]. The QT-RR adaptation time lag, measured in response to sudden heart rate (or RR interval) changes using different strategies, has been shown to provide information on the risk of arrhythmic complications and SCD [13]. In particular, a prolonged QT adaptation time has been associated with a higher probability of dying from arrhythmic causes [14]–[17]. Other ECG markers related to malignant ventricular arrhythmias include those quantifying T wave characteristics [8], such as the width of the T wave [18], the relation between the T peak-to-T end and the RR intervals [19], and the time and amplitude variability of the T wave with the RR interval quantified by metrics derived from time warping [20], [21]. Periodic depolarization dynamic (PRD) is another technique analyzing the depo-to-repo variability [22] mediated by the ventricular sympathetic innervation.

We recently proposed a model-based method to estimate

This work is licensed under a Creative Commons Attribution 4.0 License. For more information, see https://creativecommons.org/licenses/by/4.0/

This article has been accepted for publication in IEEE Transactions on Biomedical Engineering. This is the author's version which has not been fully edited and content may change prior to final publication. Citation information: DOI 10.1109/TBME.2025.3607144

the QT-RR adaptation time lag from ECGs recorded during an exercise stress test (EST) [23]. This methodology was proposed as an alternative to those that require sudden RR changes because gradual changes in heart rate are always observed during EST, resulting in a less strenuous maneuver, in contrast to sudden changes in the RR interval which are less frequently seen in Holter recordings used in the studies mentioned previously. In [23] The QT-RR time lag was estimated as the delay between the observed QT interval series and the instantaneous QT interval series derived from the RR intervals using a QT-RR regression formula (QT-based strategy). The parameters of the regression were estimated using [QT, RR] data pairs taken from three different learning windows along EST: one taken in the rest phase before the EST started (W_b), another at the end of the EST, which corresponds to a rest area at the late recovery phase (W_{lr}), and the last was selected centered on the peak exercise (W_e). Rest phases were defined as areas in which the mean heart rate does not change much, that is, the RR series can be assumed to be stationary.

The results in [23] indicated that a prolonged QT-RR adaptation time lag during the exercise phase of the EST and a shortened lag during the recovery phase were associated with a higher risk of CAD. Furthermore, the difference between QT-RR adaptation time lags in the exercise and recovery phases was significantly greater in low-risk patients compared to high-risk patients.

Additionally, we demonstrated that modifying the QT values in the [QT, RR] data pairs within the peak exercise learning window W_e helps mitigate the non-stationarity of the [QT, RR] pairs. This modification involves the replacement of the QT values with modified instantaneous QT interval values. The latter incorporates the expected evolution of QT interval if sufficient time had been given for it to converge to the corresponding RR intervals. This leads to more accurate estimates of the patient-specific QT-RR regression formula [24].

In this context, the present study introduces two key innovations. First, we propose and validate a novel method to estimate the QT-RR adaptation time lag, which reverses the conventional modeling approach by using the QT interval to predict the RR interval. We hypothesized that this strategy offers greater robustness due to the wider dynamic range of the RR series during an EST. Second, we demonstrate the SCD and cardiovascular death (CVD) risk predictive value of some of the proposed markers (QT-RR adaptation time lag estimated in exercise and recovery phases, separately, and the difference between them) in a large cohort of CAD patients.

The structure of the paper is as follows. Section II introduces the clinical dataset, the QT-RR model that relates the observed QT series with the observed RR series, and the method to estimate the QT adaptation time lag. Sections III and IV present and discuss the results, respectively, and Section V provides the main conclusions.

II. Methods

A. Database

The ARTEMIS study collected patients with CAD who underwent coronary angiography at the Division of Cardiology at Oulu University Hospital, Oulu, Finland [25] (ClinicalTrials.gov identifier NCT1426685). Patients who met the criteria for prophylactic implantation of ICD, including all with left ventricular ejection fraction $<35\%$, were excluded from the study regardless of whether an ICD was implanted. The study was carried out according to the Declaration of Helsinki and with the approval of the institutional ethics committee of research ethics of the Northern Ostrobothnia Hospital District [25]. All subjects provided written informed consent. An incremental symptom-limited maximal EST on a bicycle ergometer was implemented. The work rate was increased by 15 W in men and 10 W in women every minute from an initial 30 W workload. The test started in a supine resting position, followed by an exercise phase until peak exercise and finally a 1-2 minute post-exercise phase without a cooldown period. The study population comprised 1886 8-lead standard ECGs recorded during EST. Of these, 1472 recordings were analyzed after excluding those with the absence of rest phases at the beginning or end of the EST, poor general ECG quality or poor T wave signal-to-noise ratio and presence of large areas with non-sinus rhythm. The mean follow-up time was 8.9 years.

Patients were classified as a function of their degree of CAD according to the SYNTAX score (*SXscore*), whose value was calculated by evaluating each coronary lesion with diameter stenosis $\geq$50% in vessels $\geq$1.5 mm. The low-risk (SXscore-LR), mild-risk (SXscore-MR) and high-risk (SXscore-HR) SXscore groups were defined as [26]:

- SXscore-LR: $\mathit{SXscore} < 23$
- SXscore-MR: $23 \leq \mathit{SXscore} < 33$
- SXscore-HR: $33 \leq \mathit{SXscore}$.

The number of patients in each group was 1128, 136 and 93, respectively. The *SXscore* values were not available for 115 patients from the 1472 patients.

The primary endpoint in this study was SCD or resuscitation from sudden cardiac arrest (SCA), whichever occurred first. Secondary endpoints included any CVD. The cause of death was defined by an endpoint committee based on death certificates, interviews with the closest relatives of victims and autopsy reports. The study population included 49 patients with SCD and 63 patients with CVD, of which 11 and 12 were women, respectively.

The typical EST is characterized by the presence of four distinct phases. The initial phase, also known as the rest or basal phase, occurs before any alterations in workload. This is followed by the exercise and recovery phases, which correspond to the physical exertion and subsequent recovery periods, respectively. The final phase, known as the late recovery phase, corresponds to a period of rest that follows the recovery phase [24].

Demographic variables, the median heart rate, and QT interval values at window W_b defined at the beginning of the test, at peak exercise window W_e, and at window W_{lr} defined at the end of late recovery phase for each *SXscore* group are shown in Table I. The method for choosing the duration of these windows is described in Section II-B.

This work is licensed under a Creative Commons Attribution 4.0 License. For more information, see https://creativecommons.org/licenses/by/4.0/

This article has been accepted for publication in IEEE Transactions on Biomedical Engineering. This is the author's version which has not been fully edited and content may change prior to final publication. Citation information: DOI 10.1109/TBME.2025.3607144

TABLE I: Demographic information in patient groups including heart rate (HR) and QT interval median values ($\pm$ interquartile range), in windows W_j, $j \in \{b, e, lr\}$, denoted HR^{W_j} and QT^{W_j}, respectively. The number of Cardiovascular Death (CVD) and Sudden Cardiac Death (SCD) victims in each group is also included.

Clinical variables					
	SXscore-LR	SXscore-MR	SXscore-HR	Not available	p-value
Gender [M/All]	753/1128	103/136	74/93	91/115	0.004
Age (years)	66.0 ± 11.0	68.0 ± 12.0	68.0 ± 11.0	69.0 ± 10.0	< 0.001
BMI (kg/m^2)	27.0 ± 5.0	27.0 ± 5.3	27.0 ± 4.0	28.0 ± 5.4	0.576
CVD (SCD)	34 (34)	7 (3)	9 (4)	13 (8)	< 0.001 (0.130)
ECG-derived variables					
	SXscore-LR	SXscore-MR	SXscore-HR	Not available	p-value
HR^{W_b}(bpm)	59.6 ± 12.1	58.5 ± 9.6	61.0 ± 14.7	59.5 ± 11.0	0.113
HR^{W_e}(bpm)	126.1 ± 29.3	115.0 ± 26.9	114.8 ± 31.5	106.8 ± 25.2	< 0.001
$\text{HR}^{W_{lr}}$(bpm)	75.5 ± 14.4	70.7 ± 14.4	73.01 ± 15.3	70.3 ± 13.2	< 0.001
QT^{W_b}(ms)	415.8 ± 41.0	421.9 ± 33.0	418.0 ± 46.0	423.1 ± 33.6	0.082
QT^{W_e}(ms)	303.7 ± 41.4	317.4 ± 42.0	320.7 ± 47.0	335.0 ± 45.8	< 0.001
$\text{QT}^{W_{lr}}$(ms)	391.6 ± 38.6	400.0 ± 34.3	402.0 ± 44.0	408.0 ± 36.4	< 0.001

Results are statistically significant ($p < 0.05$) between pairs of groups SXscore-LR/SXscore-MR and SXscore-LR/SXscore-HR for *age*, HR^{We}, $\text{HR}^{W_{lr}}$, QT^{We} and $\text{QT}^{W_{lr}}$.

B. QT-RR modeling

In a previous work, we defined a procedure to estimate the QT-RR adaptation time lag using the observed $d_{\text{RR}}(n)$ series of ECGs recorded during EST as input of the QT-RR modeling [24]. In that model, the QT-RR adaptation time lag was estimated as the delay between the observed QT interval series $d_{\text{QT}}(n)$ and an instantaneous series $d^i_{\text{QT}}(n)$, related to the series $d_{\text{RR}}(n)$ through a memoryless transformation; see Fig. 1(a). This strategy is referred to as QT-based strategy.

A differentiable hyperbolic function

$$d^i_{\text{QT}}(n) = g_f\left(d_{\text{RR}}(n); \alpha, \beta\right) = \beta + \frac{\alpha}{d_{\text{RR}}(n)} \qquad (1)$$

was used in the first block to account for the calculation of the instantaneous series $d^i_{\text{QT}}(n)$. The α and β parameters of the model were estimated using the [QT, RR] data pair information from the three learning windows W_b, W_e and W_{lr}. An example of the RR and QT series computed from an ECG recorded during an EST and the location of the three learning windows are shown in Fig. 2(a).

Motivated by the fact that the series $d_{\text{RR}}(n)$ exhibits a wider dynamic range than the series $d_{\text{QT}}(n)$ during EST, as can be observed in Fig. 2(b), in this study we alternatively proposed to revert the model in Fig. 1(a) to use the series $d_{\text{QT}}(n)$ as input and estimate the delay from the series related to $d_{\text{RR}}(n)$. The new modeling strategy proposed in this study is shown in Fig. 1(b), and can be derived by a direct inversion of the model used in [27]. Note that the two system blocks in Fig. 1(b) are in reverse order to what a direct model inversion of the model in Fig. 1(a) would have given. Since $g(\cdot)$ function is non-linear, this block reversal is not generally acceptable. However, it has been proved that for typical RR interval dynamics, the effective system memory –length of $h(n)$– allows to consider the RR interval during this length to vary in a range where the $g(\cdot)$ function can be approximated as linear [24]. Under these conditions, the two system blocks, and thus the two models in Fig. 1, become interchangeable.

With this alternative model, the estimation of the QT-RR adaptation time lag was calculated as the delay between the observed RR intervals $d_{\text{RR}}(n)$ and a memoryless

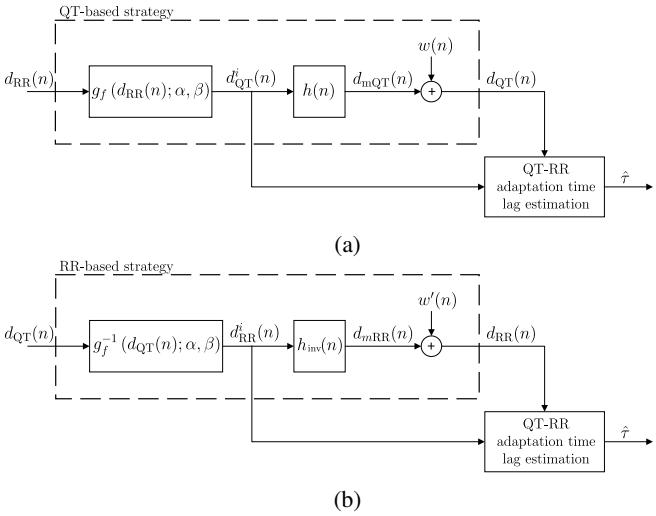

Fig. 1: (a) Model relating the observed RR series $d_{\text{RR}}(n)$ to the observed QT series $d_{\text{QT}}(n)$ [24]. The intermediate generated output of the memoryless transformation $g\left(d_{\text{RR}}(n); \alpha, \beta\right)$ is an instantaneous QT series $d^i_{\text{QT}}(n)$ that, when filtered by a single-pole lineal filter $h(n)$, models the QT series $d_{\text{mQT}}(n)$. The observed $d_{\text{QT}}(n)$ is modeled as the sum of $d_{\text{mQT}}(n)$ and noise $w(n)$. The QT-RR adaptation time lag τ is estimated as the delay between $d^i_{\text{QT}}(n)$ and $d_{\text{QT}}(n)$, referred to as QT-based strategy. (b) Reverted model relating the observed QT series $d_{\text{QT}}(n)$ to the observed RR series $d_{\text{RR}}(n)$. The generated output of the memoryless transformation $g^{-1}\left(d_{\text{QT}}(n); \alpha, \beta\right)$ is now the instantaneous RR series $d^i_{\text{RR}}(n)$ that, when filtered by a linear, time-invariant, anti-causal, filter $h_{\text{inv}}(n)$, models the RR series $d_{\text{mRR}}(n)$. The observed $d_{\text{RR}}(n)$ is modeled as the sum of $d_{\text{mRR}}(n)$ and noise $w'(n)$. The QT-RR adaptation time lag τ is estimated as the delay between $d^i_{\text{RR}}(n)$ and $d_{\text{RR}}(n)$, referred to as RR-based strategy.

series $d^i_{\text{RR}}(n)$ related to the observed QT intervals $d_{\text{QT}}(n)$ by the inverse memorylees transformation $g_f^{-1}(\cdot)$, referred as to RR-based strategy. Note that for sufficient low-frequency

This work is licensed under a Creative Commons Attribution 4.0 License. For more information, see https://creativecommons.org/licenses/by/4.0/

This article has been accepted for publication in IEEE Transactions on Biomedical Engineering. This is the author's version which has not been fully edited and content may change prior to final publication. Citation information: DOI 10.1109/TBME.2025.3607144

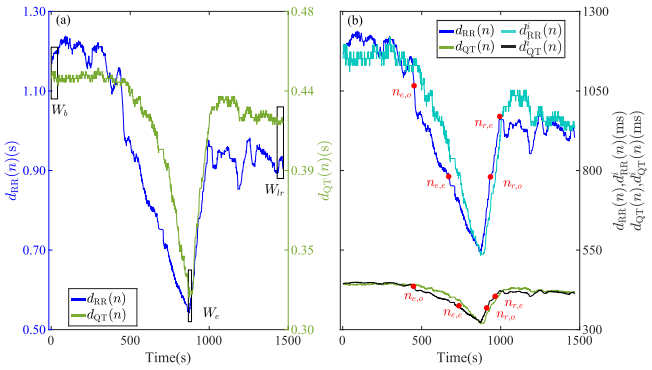

Fig. 2: (a) An observed RR series, $d_{\text{RR}}(n)$, and QT series, $d_{\text{QT}}(n)$, are presented together with the learning windows positioned at rest W_b, peak exercise W_e and late recovery W_{lr}, which are indicated by boxes. (b) The observed QT series $d_{\text{QT}}(n)$ (green line) overplotted with the related instantaneous QT series $d^i_{\text{QT}}(n)$ (black line) are shown, where the intervals for time lag estimation are delimited by $n_{e,o}$ and $n_{e,e}$ for exercise and $n_{r,o}$ and $n_{r,e}$ for recovery. The observed RR series $d_{\text{RR}}(n)$ (blue line) and the related instantaneous RR series $d^i_{\text{RR}}(n)$ (light blue line) are also represented, showing clearly the differences in dynamic range of the series during EST.

components of QT trend oscillations, filter $h(n)$ can be well approximated by a pure delay system [24], so its inverse filter $h_{\text{inv}}(n)$ becomes a pure advance filter. We hypothesized that this RR-based strategy for the calculation of the QT-RR time lag could offer improved estimation performance as a result of the larger dynamic range of the RR series as compared to the QT series during EST. Thus, the series $d^i_{\text{RR}}(n)$ was delayed with respect to $d_{\text{RR}}(n)$.

Therefore, the differentiable function

$$d^i_{\text{RR}}(n) = g_f^{-1}\left(d_{\text{QT}}(n); \alpha, \beta\right) = \frac{\alpha}{d_{\text{QT}}(n) - \beta} \tag{2}$$

was used in the first block to account for the calculation of the memoryless series $d^i_{\text{RR}}(n)$. The series $d^i_{\text{RR}}(n)$ kept the same temporal variation as $d_{\text{QT}}(n)$, but its values were comparable to those of the series $d_{\text{RR}}(n)$.

The two scalar parameters α and β were estimated previously to the QT-RR model, independently for each patient, using [QT, RR] data pairs from the three learning windows. Two of the windows were defined in the RR assumed stationary areas at the first 40 s of baseline rest before exercise W_b and at the last 40 s of late recovery W_{lr}, respectively, where the series are assumed to be stationary. The third window was centered at peak exercise W_e with a length of 20 s, taking the last 10 s of exercise and the first 10 s of recovery. The window at peak exercise was taken to include the greatest possible range of [QT, RR] values when estimating the model parameters. However, data in W_e window is far from a steady state. Consequently, the [QT, RR] pairs may not show the same relation as they would in a stationary state, as is required for model parameter identification [24]. To account for the lack of stationarity, the QT interval values within the W_e window were modified using a first QT–RR adaptation time lag estimated in the exercise phase, $\hat{\tau}_e$. By combining $\hat{\tau}_e$ with the estimated rate of change of the QT interval at peak exercise, denoted by s, we derive new modified QT values based on a stationarity approach. Specifically, if stationarity had been reached, these new values would be expressed as QT-$(s \cdot \hat{\tau}_e)$. Consequently, new estimates of the parameters of the model were performed using the data pairs [QT-$(s \cdot \hat{\tau}_e)$, RR] at W_e, see [23], [24] for details. Therefore, this new series was denoted as $\check{d}^i_{\text{RR}}(n)$ or $\check{d}^i_{\text{QT}}(n)$, depending on the modeling strategy used (see [24] for a detailed analysis). Concatenated series in windows $W_b \cup W_e \cup W_{lr}$ (before or after modifying peak exercise window W_e) should contain a wide range of RR or QT values to produce a more reliable least-squares fit that ensures the best estimation of model parameters. Data from window We were replicated twice to ensure the three regions were equally weighted in the estimation of the model parameters α and β.

C. QT-RR adaptation time lag estimation

The right part of the proposed model in Fig. 1(b) represents the RR-based strategy for QT-RR adaptation time lag estimation, which considers the observed RR interval series $d_{\text{RR}}(n)$ and the instantaneous series $\check{d}^i_{\text{RR}}(n)$.

A Laplacian estimator [28], [29] was used to compute the delay between the time series $d_{\text{RR}}(n)$ and $\check{d}^i_{\text{RR}}(n)$ in exercise and recovery phases, $\check{\tau}_e$ and $\check{\tau}_r$, independently:

$$\check{\tau}_x = \arg \min_{-I \le \tau \le I} \sum_{n=n_a}^{n_b} |d_{\text{RR}}(n) - \check{d}^i_{\text{RR}}(n+\tau)|, \; x \in \{e, r\} \tag{3}$$

where the delay $\check{\tau}$ was restricted to be contained in the search range $[-I, I]$. Thus, the maximum likelihood estimator was identical to minimizing the least absolute error between $d_{\text{RR}}(n)$ and $\check{d}^i_{\text{RR}}(n+\tau)$, in RR-based strategy. Changing $d_{\text{RR}}(n)$ and $\check{d}^i_{\text{RR}}(n+\tau)$, for $d_{\text{QT}}(n)$ and $\check{d}^i_{\text{QT}}(n-\tau)$, respectively, we obtain the estimates with QT-based strategy. The minimization interval $[n_a, n_b]$ was determined using the methodology proposed in [23]. These points define the onset and the end of the exercise and the recovery areas, separately, and they were calculated for each RR and QT series. Figure 2(b) illustrates those onsets and ends of the intervals used for estimating the time lags during exercise and recovery, separately.

The difference between $\check{\tau}_r$ and $\check{\tau}_e$ was also computed, which resulted in the third evaluated marker, $\Delta\check{\tau}$.

Furthermore, for comparison purposes, the markers $\check{\tau}_e$, $\check{\tau}_r$ and $\Delta\check{\tau}$ were also computed using the QT-based strategy, the model of which is represented in Fig. 1(a) [24].

Calculating the marker $\check{\tau}_e$ with the RR-based strategy (or QT-based strategy) required an initial estimate of $\hat{\tau}_e$ to correct the learning pairs of the [QT, RR] data at W_e [24], as previously noted in Sec. II-B. This estimated $\hat{\tau}_e$, obtained by learning the model parameters with the raw [QT, RR] data pairs at W_e, could take non-physiologically plausible values (negative, or lower than 20 s), leading to erroneous [QT, RR] data pairs modification for the estimation of $\check{\tau}_e$. To mitigate this problem and reduce the number of non-physiological values of $\hat{\tau}_e$, the following rule was introduced. When $\hat{\tau}_e < 20s$, $\hat{\tau}_e$ was replaced by a value between 20 s

This work is licensed under a Creative Commons Attribution 4.0 License. For more information, see https://creativecommons.org/licenses/by/4.0/

This article has been accepted for publication in IEEE Transactions on Biomedical Engineering. This is the author's version which has not been fully edited and content may change prior to final publication. Citation information: DOI 10.1109/TBME.2025.3607144

and 70 s, chosen as the minimum value within this range that allowed obtaining a $\check{\tau}_e$ value equal or higher than 20 s. The reference value of 20 s for $\hat{\tau}_e$ corresponded to the lowest $\hat{\tau}_e$ obtained in a previous study using a different low-risk CAD patients dataset [23]. In cases in which the search did not provide any results, $\hat{\tau}_e$ was set to 20 s. This rule allowed us to compute a $\check{\tau}_e$ in all the cases.

D. Comparison of QT-based strategy to RR-based strategy in simulated ECGs

In this work, we reproduced the simulation study from [24], which generates EST ECGs with specific τ values corresponding to given signal-to-noise ratios (SNR). The idea was to compare the estimated adaptation time lag using either the RR- or the QT-based strategy in a controlled environment, as simulated EST ECGs, in which the true adaptation time was known. Moreover, the robustness of each strategy was also evaluated using simulated EST ECGs with different SNR.

Two of the three ECG subsets used in [24] were selected and grouped to assess the improvement in QT-RR adaptation time lag estimation when the RR-based strategy is applied. The first ECG subset consists of simulated EST ECG generated using linear transition trends of the mean heart rate when moving from rest to peak exercise and from peak exercise to late recovery. This subset was denoted as $\mathcal{D}_t$ in [24]. The second subset, denoted as $\mathcal{D}_r$, was generated using 25 different EST heart rate series extracted from real EST ECGs (see [24] for details).

In total, the simulated EST ECG dataset used in this study consists of 50 ECGs (25 from $\mathcal{D}_t$ and 25 from $\mathcal{D}_r$), for all possible combinations of τ and SNR, assuming the following values:

$$\tau = \{20, 30, 40, 50\} \text{ s}, \tag{4}$$

$$\text{SNR} = \{27, 30, 35, 40\} \text{ dB}, \tag{5}$$

where the different SNRs correspond to the following root mean square noise values: $\{45, 32, 18, 10\}$ μV, resulting in a total of $50 \cdot 4 \cdot 4 = 800$ EST ECGs.

The QT-RR adaptation time lag estimation performance was quantified by the error ϵ_τ between the estimated time lag $\check{\tau}_x$, $x \in \{e, r\}$, and the true time lag τ,

$$\epsilon_\tau(x) = \check{\tau}_x - \tau, \tag{6}$$

The results are expressed in terms of mean bias m_{ϵ_τ} and standard deviation σ_{ϵ_τ} of the time lag error ϵ_τ computed over the entire simulated ECG dataset, and presented separately for exercise and recovery.

E. Statistical Analysis

All clinical data values were presented as median $\pm$ interquartile range (IQR) values. The QT-RR adaptation time lag estimates were represented in box plot diagrams, in which both the mean and median values were displayed. Estimates were also presented as mean $\pm$ standard deviation values along the text to allow numerical comparison with data from other studies.

In multiple comparisons, the Kruskal-Wallis test was used to assess differences in continuous clinical variables and ECG-derived variables.

The Mann-Whitney U test was applied for the comparison of continuous variables, such as the three proposed markers $\check{\tau}_e$, $\check{\tau}_r$ and $\check{\Delta}\tau$, between groups. The Chi-square test was applied to assess differences in the categorical variable gender. $p < 0.05$ was chosen to considered statistical significance.

Univariable and multivariable Cox regression analyses were performed to independently determine the predictive value of risk markers for the two primary endpoints, i.e. SCD and CVD. Only variables with significant individual association with the endpoint in the univariable analysis were included to define the multivariable model. The C-index was used to evaluate the detection performance of the model. A backward stepwise regression analysis was performed to optimize the model and retain only the independent variables associated with the endpoint. Hazard ratio ($\mathcal{HZR}$) results are presented per increment/decrement of one IQR, with such hazard ratio denoted as $\mathcal{HZR}_{\text{IQR}}$ or, in some cases, per increments of k units of the variable, denoted as $\mathcal{HZR}_k$.

III. Results

A. Evaluation in simulated ECGs

Mean error m_{ϵ_τ} and standard deviation σ_{ϵ_τ} values computed from the simulated ECG dataset are displayed in Fig. 3 for the QT-based strategy and RR-based strategy, separately. It can be observed that the mean error is closer to zero when the RR-based strategy is implemented as compared to the QT-based strategy. Besides, the standard deviation values are slightly lower when the RR-based strategy is employed. These observations support the hypothesis that more robust estimates should be obtained using the RR-based strategy.

B. Clinical characteristics

Demographic information for each group of patients, together with the median of the heart rate and the QT intervals at basal, peak exercise and late recovery windows W_j, $j \in \{b, e, lr\}$, HR_{W_j} and QT_{W_j}, respectively, is given in Table I. The median age and BMI and the proportion of males vs females were higher in the groups with higher *SXscore*. Note that the median heart rate at peak exercise, HR^{W_e}, decreased significantly with increasing *SXscore*.

The capacity of the proposed markers $\check{\tau}_e$, $\check{\tau}_r$ and $\check{\Delta}\tau$, estimated using either the QT-based strategy or the RR-based strategy, for CAD stratification and SCD prediction, was evaluated. Patients resulting in either negative $\check{\tau}_e$ or negative $\check{\tau}_r$ were removed from the analysis due to their non-physiological interpretation.

C. QT-RR adaptation time lag for CAD stratification

In this section, the statistical potential of the proposed markers to stratify patients with different *SXscore* is evaluated. First, the QT adaptation time lags were estimated following the QT-based strategy. The results are presented in the first

This work is licensed under a Creative Commons Attribution 4.0 License. For more information, see https://creativecommons.org/licenses/by/4.0/

This article has been accepted for publication in IEEE Transactions on Biomedical Engineering. This is the author's version which has not been fully edited and content may change prior to final publication. Citation information: DOI 10.1109/TBME.2025.3607144

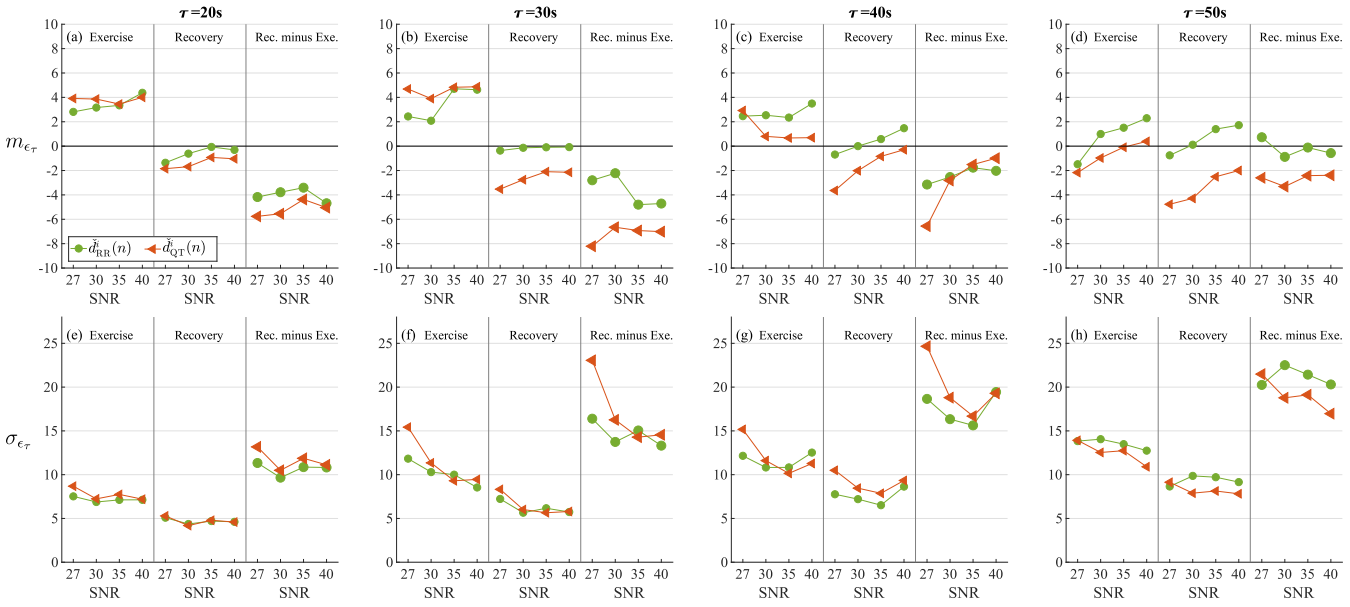

Fig. 3: Mean m_{ϵ_τ} and standard deviation σ_{ϵ_τ} of the time lag error ϵ_τ calculated from simulated ECGs with different values of τ (columns) and SNRs (horizontal axis) are shown in (a)–(d) and (e)–(h), respectively. Results were computed in exercise, in recovery and as the difference between these estimated time lags. Results are obtained using the RR-based strategy (green) and QT-based strategy (orange), separately.

column of Fig. 4. SXscore-LR, SXscore-MR and SXscore-HR groups are finally composed of 837, 109 and 75 patients, respectively, after discarding patients with non-physiological τ. It can be seen from Fig. 4 that the highest risk group was associated with the highest values of $\check{\tau}_e$ and the lowest values of $\Delta\check{\tau}$. In addition, statistically significant differences, or borderline p-values, are obtained between SXscore-LR/SXscore-HR and SXscore-MR/SXscore-HR for the two mentioned markers. However, the distribution of the estimated $\check{\tau}_r$ values is similar along groups.

Next, the analysis was repeated following the RR-based strategy, whose results are shown in the second column of Fig. 4. In this case, SXscore-LR, SXscore-MR and SXscore-HR groups were composed of 888, 112 and 75 patients, respectively, after discarding patients with non-physiological τ. Note that the number of discarded patients is lower with the RR-based strategy than with the QT-based strategy. Statistically significant differences between the *SXscore* groups were observed for the RR-based strategy estimated delay in exercise, $\check{\tau}_e$. However, no statistical significance was observed using the other two markers.

D. QT-RR adaptation time lag for SCD risk prediction

The distribution of estimated delays for patients who suffered SCD and those who suffered CVD is represented in the box plots of Fig. 5, for delays estimated using the QT-based strategy and RR-based strategy. The number of measurable survivors and victims of SCD was 1074 and 39 when the analysis was based on the QT-based strategy, and 1128 and 37 using the RR-based strategy. For CVD, the numbers were 1060 and 53 for QT-based strategy and 1112 and 57 for RR-based strategy.

The marker $\check{\tau}_r$ could discriminate between victims and survivors of SCD when delays were estimated using the RR-based strategy (Fig. 5(e)). Patients who suffered from SCD had higher values of $\check{\tau}_r$ ($m_{\check{\tau}_r} = 53.17 \pm 27.28$ s) than those who survived to SCD ($m_{\check{\tau}_r} = 42.96 \pm 28.02$ s), with the differences being statistically significant. These statistical differences were also observed using $\Delta\check{\tau}$ (Fig. 5(f)), with $m_{\Delta\check{\tau}} = 1.78 \pm 45.26$ s for SCD survivors and $m_{\Delta\check{\tau}} = 14.05 \pm 41.21$ s for SCD victims. When the endpoint was CVD, the marker $\check{\tau}_r$ led to borderline significant differences between victims and survivors of CVD ($m_{\check{\tau}_r} = 51.62 \pm 26.10$ s and $m_{\check{\tau}_r} = 42.89 \pm 28.08$ s, respectively). Similar behavior was observed when $\check{\tau}_r$ was calculated using the QT-based strategy (Fig. 5(b)).

The univariable and multivariable Cox analyses for SCD and CVD prediction are summarized in Table II and Table III, respectively. The median QT_c values for the learning windows W_j, $j \in \{b, e, lr\}$, were computed using the Fridericia correction [30] and were included in the predictive models.

The best univariable model for SCD was obtained with QT^{W_e} (C-index close to 0.70), calculated using either the QT-based strategy or the RR-based strategy. The observed differences can be attributed to the slight variation in the patient population under study. In contrast, the best univariable model for CVD was obtained with HR^{W_e} (C-index = 0.73) calculated using the QT-based strategy and with HR^{W_e} or QT^{W_e} (C-index = 0.73) calculated using the RR-based strategy.

The proposed marker $\check{\tau}_r$ was associated with both SCD and CVD when the delay was estimated using the RR-based strategy, with a C-index equal to 0.62 and 0.57, respectively. The corresponding values of $\mathcal{HZR}$ were $\mathcal{HZR}_{\mathrm{IQR}}$ equal to 1.55 (95%, CI 1.05-2.30) and 1.44 (95%, CI

This work is licensed under a Creative Commons Attribution 4.0 License. For more information, see https://creativecommons.org/licenses/by/4.0/

This article has been accepted for publication in IEEE Transactions on Biomedical Engineering. This is the author's version which has not been fully edited and content may change prior to final publication. Citation information: DOI 10.1109/TBME.2025.3607144

TABLE II: Univariable and multivariable association with sudden cardiac death.

Series	$\tilde{d}^i_{\mathrm{QT}}(n)$					$\tilde{d}^i_{\mathrm{RR}}(n)$				
Risk factor	**median ± IQR or count**	**Univariable analysis**		**Multivariable analysis**		**median ± IQR or count**	**Univariable analysis**		**Multivariable analysis**	
		$\mathcal{HZR}_{\mathrm{IQR}}$ (95% CI)	p-value	$\mathcal{HZR}_{\mathrm{IQR}}$ (95% CI)	p-value		$\mathcal{HZR}_{\mathrm{IQR}}$ (95% CI)	p-value	$\mathcal{HZR}_{\mathrm{IQR}}$ (95% CI)	p-value
Sex (female)	385	0.46 (0.21-1.00)	0.05*	0.33 (0.15-0.72)	0.01*	384	0.45 (0.20-1.03)	0.06	...	...
Age (years)	67.0 ± 11.0	1.52 (0.96-2.39)	0.07	...	...	67.0 ± 12.0	1.35 (0.83-2.20)	0.23	...	...
BMI (Kg/m^2)	28.0 ± 5.8	1.11 (0.75-1.66)	0.60	...	...	27.0 ± 5.0	1.19 (0.84-1.67)	0.33	...	...
HR^{W_b} (bpm)	59.5 ± 11.8	1.56 (1.10-2.20)	0.01*	2.24 (1.50-3.35)	<0.01*	59.3 ± 11.7	1.43 (0.99-2.07)	0.05*	1.99 (1.32-3.00)	<0.01*
HR^{W_e} (bpm)	119.51 ± 27.9	0.40 (0.25-0.65)	<0.01*	0.32 (0.19-0.56)	<0.01*	122.5 ± 29.3	0.43 (0.26-0.71)	<0.01*	0.46 (0.23-0.93)	0.03
HR$^{W_{lr}}$ (bpm)	73.0 ± 14.0	0.90 (0.60-1.35)	0.62	...	...	73.6 ± 14.3	0.84 (0.55-1.28)	0.41	...	...
QT^{W_b} (ms)	418.0 ± 39.0	1.21 (0.81-1.78)	0.35	...	...	417.9 ± 38.4	1.27 (0.85-1.88)	0.24	...	...
QT^{W_e} (ms)	313.0 ± 42.0	2.20 (1.56-3.11)	<0.01*	...	...	308.0 ± 41.6	2.06 (1.46-2.90)	<0.01*	...	...
QT$^{W_{lr}}$ (ms)	396.0 ± 38.0	1.34 (0.92-1.96)	0.13	...	...	394.0 ± 38.4	1.41 (0.96-2.07)	0.08	...	...
QT$_c^{W_b}$ (ms)	416.0 ± 28.0	1.69 (1.22-2.34)	<0.01*	1.66 (1.16-2.38)	0.01*	415.7 ± 27.0	1.69 (1.22-2.33)	<0.01*	...	..
QT$_c^{W_e}$ (ms)	392.6 ± 26.5	2.00 (1.46-2.72)	<0.01*	...	...	390.6 ± 27.1	2.01 (1.46-2.77)	<0.01*	1.50 (0.95-2.39)	0.08
QT$_c^{W_{lr}}$ (ms)	423.2 ± 25.8	1.34 (0.93-1.93)	0.11	...	...	423.0 ± 25.5	1.37 (0.95-1.99)	0.09	...	...
$\check{\tau}_e$ (s)	29.3 ± 32.5	1.08 (0.76-1.54)	0.67	...	...	34.5 ± 33.8	0.93 (0.62-1.40)	0.74	...	...
$\check{\tau}_r$ (s)	33.0 ± 27.3	1.18 (0.82-1.70)	0.37	...	...	37.5 ± 39.5	1.55 (1.05-2.30)	0.03*	1.85 (1.25-2.74)	<0.01*
$\Delta_{\check{\tau}}$ (s)	0.75 ± 48.3	1.04 (0.71-1.52)	0.85	...	...	1.5 ± 54.5	1.39 (0.93-2.07)	0.11	...	...
C-index	0.69 (with QT^{W_e})			0.80		0.68 (with QT^{W_e})			0.75	

HR = heart rate, W_b = learning window defined in the first basal phase, W_e = learning window defined at peak exercise, W_{lr} = learning window defined in the late recovery phase.
* Note that differences in values between $d^i_{\mathrm{QT}}(n)$ and $d^i_{\mathrm{RR}}(n)$ columns for variables not related with τ in the univariable analysis are due to the different rejection patient set when calculating both series.

TABLE III: Univariable and multivariable association with cardiovascular death.

Series	$\tilde{d}^i_{\mathrm{QT}}(n)$					$\tilde{d}^i_{\mathrm{RR}}(n)$				
Risk factor	**median ± IQR or count**	**Univariable analysis**		**Multivariable analysis**		**median ± IQR or count**	**Univariable analysis**		**Multivariable analysis**	
		$\mathcal{HZR}_{\mathrm{IQR}}$ (95% CI)	p-value	$\mathcal{HZR}_{\mathrm{IQR}}$ (95% CI)	p-value		$\mathcal{HZR}_{\mathrm{IQR}}$ (95% CI)	p-value	$\mathcal{HZR}_{\mathrm{IQR}}$ (95% CI)	p-value
Sex (female)	385	0.37 (0.18-0.76)	0.01*	0.27 (0.13-0.55)	<0.01*	384	0.40 (0.20-0.82)	0.01*	0.29 (0.14-0.59)	<0.01*
Age (years)	67.0 ± 11.0	3.41 (2.19-5.30)	<0.01*	2.37 (1.48-3.79)	<0.01*	67.0 ± 12.0	3.46 (2.18-5.50)	<0.01*	2.22 (1.34-3.65)	<0.01*
BMI (Kg/m^2)	28.0 ± 5.8	0.92 (0.63-1.32)	0.64	...	...	27.0 ± 5.0	1.02 (0.75-1.39)	0.88	...	...
HR^{W_b} (bpm)	59.5 ± 11.8	1.05 (0.74-1.48)	0.80	...	...	59.3 ± 11.7	1.10 (0.78-1.54)	0.59	...	...
HR^{W_e} (bpm)	119.51 ± 27.9	0.27 (0.17-0.42)	<0.01*	0.33 (0.21-0.53)	<0.01*	122.5 ± 29.3	0.27 (0.17-0.42)	<0.01*	0.31 (0.20-0.50)	<0.01*
HR$^{W_{lr}}$ (bpm)	73.0 ± 14.0	0.56 (0.39-0.81)	<0.01*	...	...	73.6 ± 14.3	0.52 (0.36-0.76)	<0.01*	...	...
QT^{W_b} (ms)	418.0 ± 39.0	1.33 (0.96-1.85)	0.09	...	...	417.9 ± 38.4	1.30 (0.93-1.80)	0.12	...	...
QT^{W_e} (ms)	313.0 ± 42.0	2.43 (1.83-3.24)	<0.01*	...	...	308.0 ± 41.6	2.38 (1.81-3.13)	<0.01*	...	...
QT$^{W_{lr}}$ (ms)	396.0 ± 38.0	1.53 (1.12-2.10)	0.01*	...	...	394.0 ± 38.4	1.61 (1.18-2.21)	<0.01*	...	...
QT$_c^{W_b}$ (ms)	416.0 ± 28.0	1.42 (1.05-1.92)	0.02*	...	...	415.7 ± 27.0	1.41 (1.06-1.89)	0.02*	...	...
QT$_c^{W_e}$ (ms)	392.6 ± 26.5	1.93 (1.48-2.51)	<0.01*	...	...	390.6 ± 27.1	2.00 (1.54-2.61)	<0.01*	...	...
QT$_c^{W_{lr}}$ (ms)	423.2 ± 25.8	1.09 (0.78-1.52)	0.61	...	...	423.0 ± 25.5	1.12 (0.80-1.56)	0.51	...	...
$\check{\tau}_e$ (s)	29.3 ± 32.5	1.14 (0.85-1.52)	0.39	...	...	34.5 ± 33.8	1.20 (0.89-1.62)	0.23	...	...
$\check{\tau}_r$ (s)	33.0 ± 27.3	1.49 (1.13-1.96)	0.01*	1.47 (1.14-1.90)	<0.01*	37.5 ± 39.5	1.44 (1.03-2.01)	0.03*	1.62 (1.17-2.25)	<0.01*
$\Delta_{\check{\tau}}$ (s)	0.75 ± 48.3	1.17 (0.84-1.64)	0.35	...	...	1.5 ± 54.5	1.21 (0.87-1.68)	0.25	...	...
C-index	0.73 (with HR^{W_e})			0.81		0.73 (with HR^{W_e} or QT^{W_e})			0.79	

HR = heart rate, W_b = learning window defined in the first basal phase, W_e = learning window defined at peak exercise, W_{lr} = learning window defined in the late recovery phase.
* Note that differences in values between $d^i_{\mathrm{QT}}(n)$ and $d^i_{\mathrm{RR}}(n)$ columns for variables not related with τ in the univariable analysis are due to the different rejection patient set when calculating both series.

1.03-2.01), respectively, resulting in $\mathcal{HZR}_{1\mathrm{s}} = 1.01$ in both cases. However, when this marker was calculated using the QT-based strategy, it was only related to CVD, with a C-index equal to 0.58. The corresponding values of $\mathcal{HZR}$ were $\mathcal{HZR}_{\mathrm{IQR}}$ equal to 1.49 (95%, CI 1.13-1.96), resulting in $\mathcal{HZR}_{1\mathrm{s}} = 1.01$. Markers $\check{\tau}_e$ and $\Delta_{\check{\tau}}$ did not yield statistically significant results.

Using the QT-based strategy, the best multivariable model for SCD prediction included sex, HR^{W_b}, HR^{W_e} and QT$_c^{W_b}$. The covariables with the greatest influence were sex, with males having a 67% increase in the risk of SCD ($\mathcal{HZR}_{\mathrm{IQR}}$ of 0.33 (95%, CI 0.15-0.72)), and HR^{W_b}, with an increment of 1 beat-pear-minute (bpm) being associated with 7% increase in the risk of SCD ($\mathcal{HZR}_{1\mathrm{bpm}} = 1.07$). Using the RR-based strategy, the best multivariable model for SCD included the variables HR^{W_b}, HR^{W_e}, QT$_c^{W_e}$ and $\check{\tau}_r$, with an increment of 1 bpm in HR^{W_b} being associated with 6% higher probability of suffering SCD ($\mathcal{HZR}_{1\mathrm{bpm}} = 1.06$), and

This work is licensed under a Creative Commons Attribution 4.0 License. For more information, see https://creativecommons.org/licenses/by/4.0/

This article has been accepted for publication in IEEE Transactions on Biomedical Engineering. This is the author's version which has not been fully edited and content may change prior to final publication. Citation information: DOI 10.1109/TBME.2025.3607144

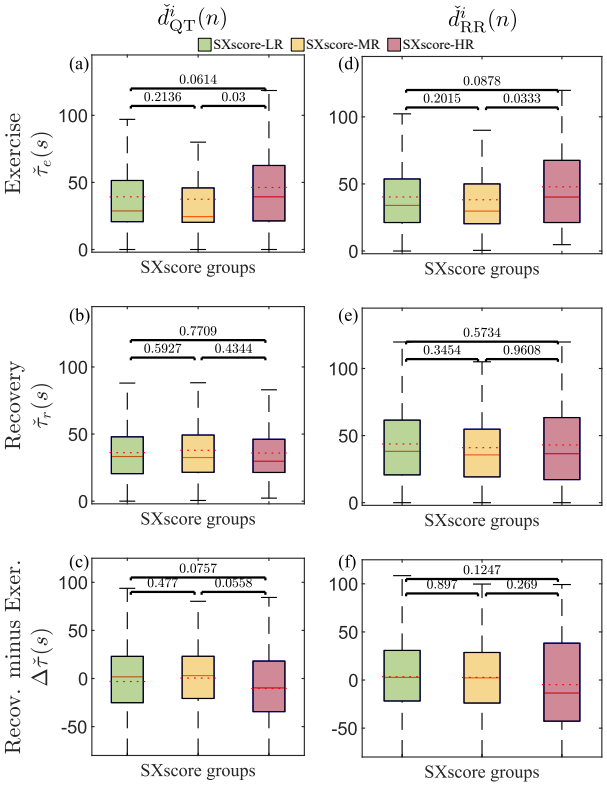

Fig. 4: First column: box plots of the estimated time delay with the QT-based strategy for (a) exercise, resulting in $\check{\tau}_e$, and (b) recovery, resulting in $\check{\tau}_r$. In (c), box plots of the difference between recovery and exercise, resulting in $\Delta\check{\tau}$ are displayed. The dotted and continuous lines in red correspond to the mean and the median values, respectively. The color code for the Syntax Score groups is: SXscore-LR (green), SXscore-MR (yellow) and SXscore-HR (red). The p-values in separating patient groups are plotted on top of the box plot pairs. The analysis was repeated for the RR-based strategy, second column, and the estimated $\check{\tau}_e$, $\check{\tau}_r$ and $\Delta\check{\tau}$ are displayed in (d), (e) and (f) graphs, respectively.

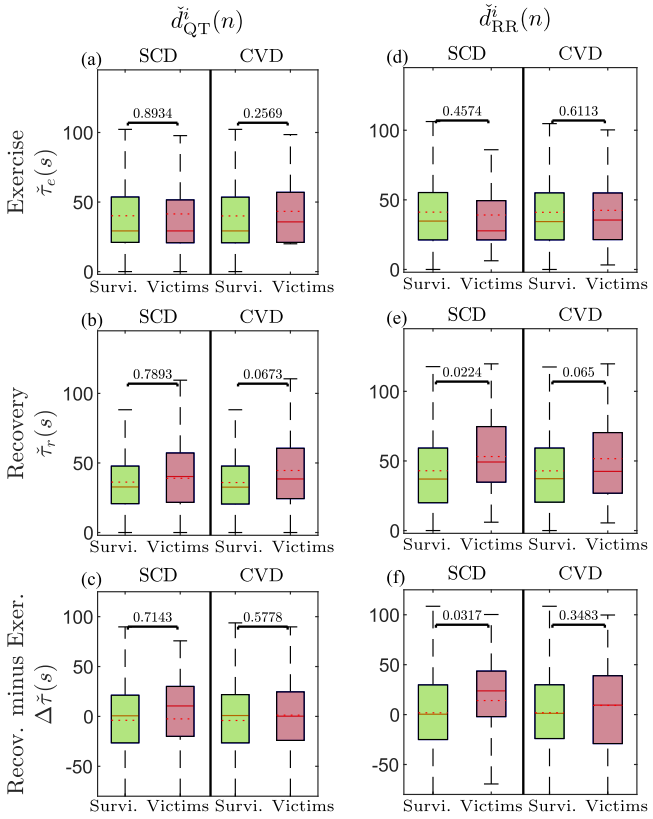

Fig. 5: First column: box plots of the estimated time delay using the QT-based strategy. The results were obtained after applying the rule to reduce the number of non-physiological τ_e estimates, which were required to compute $\check{\tau}_x$, $x \in \{e, r\}$. The estimates were obtained for (a) exercise, $\check{\tau}_e$, and (b) recovery, $\check{\tau}_r$. (c) Box plots of the difference between recovery and exercise, $\Delta\check{\tau}$. The dotted and continuous lines in red correspond to the mean and the median values, respectively. The color code is: survivors (green) and victims (red) for both SCD and CVD. The p-values in separating patient groups are overprinted on top of the box plot pairs. The analysis was repeated using the RR-based strategy, second column, whose $\check{\tau}_e$, $\check{\tau}_r$ and $\Delta\check{\tau}$ are displayed in (d), (e) and (f) graphs, respectively.

an increment of 10 s in $\check{\tau}_r$ being associated with 17% higher likelihood of suffering SCD ($\mathcal{HZR}_{10\mathrm{s}} = 1.17$).

In the case of CVD, the best multivariable model included the variables sex, age, HR^{W_e}, $\mathrm{QT}^{W_{lr}}$, $\mathrm{QT}_c^{W_b}$ and $\check{\tau}_r$, for any strategy selected to calculate the delays. An inverse relationship was found between HR^{W_e} and CVD. Men and older patients were more likely to die from CVD.

All multivariable models had a C-index greater than 0.7, suggesting that these models can stratify individuals according to their risk of SCD or CVD. The values of the C-index were higher than those of the best univariable model in each case, thus showing that the predictive accuracy is enhanced with the inclusion of additional covariables.

IV. Discussion

This work introduces several novelties, including the introduction of a reverted model, RR-based strategy, to estimate the QT adaptation time using the observed RR series. This is due to the fact that the RR series has a wider dynamic range value than their observed QT series counterpart, offering more robust estimates, as corroborated in the simulation study. In addition, the study evaluated the QT-RR adaptation time estimated from exercise stress testing ECG as a marker of SCD and CVD.

In particular, three ECG-derived markers, $\check{\tau}_e$, $\check{\tau}_r$, and $\Delta_{\check{\tau}}$, are proposed, which correspond to the adaptation time estimated during the exercise phase, the recovery phase and the difference between them, respectively. The predictive ability of these markers is also assessed using two multivariable models: one based on the QT intervals and another one based on the RR intervals.

The percentage of patients whose estimated τ_e is lower than 20 s is 53% using $d^i_{\mathrm{QT}}(n)$ (39% for $d^i_{\mathrm{RR}}(n)$). The application of the rule described in Sec.II-C allows to reduce the number of discarded patients to only 18% using $\check{d}^i_{\mathrm{QT}}(n)$ (11% for $\check{d}^i_{\mathrm{RR}}(n)$) due to non-physiological negative values of $\check{\tau}_e$. The proportion

This work is licensed under a Creative Commons Attribution 4.0 License. For more information, see https://creativecommons.org/licenses/by/4.0/

This article has been accepted for publication in IEEE Transactions on Biomedical Engineering. This is the author's version which has not been fully edited and content may change prior to final publication. Citation information: DOI 10.1109/TBME.2025.3607144

of patients with initial non-physiological estimates appears to be notably high. However, the validity of this correction rule is supported by previous simulation studies [24], which demonstrated that applying the rule yields adaptation time estimates closer to the known ground-truth values. Since the true adaptation time cannot be determined from patient data, this simulation study suggests that the rule strengthens, rather than compromises, the final estimates and their validity for risk stratification.

A. QT-RR adaptation time lag and its power for SCD risk prediction

The main finding is the relevance of the proposed marker $\check{\tau}_r$ for (a) stratifying survivors and victims of SCD or CVD, and (b) defining multivariable regression models to predict SCD or CVD when the QT-RR adaptation time lag is estimated between the series $\check{d}^i_{\mathrm{RR}}(n)$ and $d_{\mathrm{RR}}(n)$, that is, using the RR-based strategy. When the recovery time lag is estimated between $\check{d}^i_{\mathrm{QT}}(n)$ and $d_{\mathrm{QT}}(n)$, that is, using the QT-based strategy, the recovery time can only predict CVD. Thus, using the RR-based strategy is more advantageous from a clinical perspective both for the separation of CAD groups and for the prediction of SCD or CVD.

From a methodological perspective, a detailed analysis of Fig. 3 aligns with previous findings, showing that the RR-based strategy outperforms the QT-based strategy in estimating the QT-RR adaptation time. The RR-based strategy consistently exhibits lower mean error and reduced variance, particularly at low SNR values. This advantage becomes increasingly pronounced as the values of τ—which are associated with cardiovascular risk—increase, supporting the superior clinical stratification power of the RR-based strategy. At high SNR values, the improvement in both mean error and variance is less significant, reflecting the reduced impact of the larger dynamic range of the RR series compared to the QT series when both signals are cleaner. Nonetheless, for $\tau = 50$ and high SNR, the RR-strategy still shows a visible performance benefit

The importance of the marker $\check{\tau}_r$ estimated by the RR-based strategy is observed not only in univariable but also in multivariable analyses, since this variable is part of the best models to predict SCD and CVD. An increase of 10 s in $\check{\tau}_r$ leads to a 17% increase in the risk of SCD and a 12% increase in the risk of dying from CVD.

In addition, other demographic variables, such as sex, and other ECG-derived interval variables measured during peak exercise, such as HR^{W_e} and QT^{W_e}, show a strong correlation with the two investigated endpoints.

The multivariable Cox regression model for predicting CVD has also been studied using only sex, age, HR^{W_e}, $\mathrm{HR}^{W_{lr}}$ and $\check{\tau}_r$ variables, that is, removing any variable related to the QT interval. Using information derived from the RR-based strategy, the final multivariable model after applying the Akaike criterion is composed of the variables HR^{W_e} and $\mathrm{HR}^{W_{lr}}$, with their associated hazard ratios $\mathcal{HZR}_{\mathrm{IQR}}$ being 0.22 (95%, CI 0.12-0.42) and 1.50 (95%, CI 0.90-2.50), respectively. In this multivariable model, a direct relation between $\mathrm{HR}^{W_{lr}}$ variable and CVD can be observed, with higher values of $\mathrm{HR}^{W_{lr}}$ corresponding to higher mortality risk. However, the $\mathcal{HZR}$ of this variable in the univariable model is below one ($\mathcal{HZR}_{\mathrm{IQR}}$ of 0.52 (95%, CI 0.36-0.76)), thus presenting an inverse relationship with mortality risk (see Table III). Taken together, our results should be interpreted in light of the changes in different variables. Particularly in the case of $\mathrm{HR}^{W_{lr}}$, they should be interpreted in light of the changes in HR^{W_e}. From the multivariable analysis, our results show that, when $\mathrm{HR}^{W_{lr}}$ increases for a given HR^{W_e}, the risk of CVD increases.

Clinically, it could mean that patients with a higher mortality risk achieve an elevated HR in the rest area after recovery, so they cannot completely recover or have a high heart rate at rest. In terms of RR series, the risk of CVD increases when $\mathrm{RR}^{W_{lr}}$ decreases for a given RR^{W_e}. This analysis can also explain the opposite tendency of the $\mathcal{HZR}$ value of $\mathrm{QT}^{W_{lr}}$ obtained in the multivariable regression model in Table III, as compared to the univariable model.

Some considerations related to Cox analysis should be noted. First, the *SXscore* information is not included because a nonsignificant relationship was found between this variable and any of the two investigated endpoints. Second, a standardization of the variables was performed based on their median and IQR after observing that not all variables followed a normal distribution. Dichotomizing the variables would have been another option. This would require setting a threshold on e.g. $\check{\tau}_r$, which has not been studied in the literature yet.

B. Clinical implications

Prior studies [21], [31], [32] have emphasized that increased spatio-temporal variability in T-wave morphology and QT intervals reflects elevated arrhythmogenic risk, and these ECG-derived markers are independent predictors of SCD. However, the dispersion and variability studied in most of these works have been analyzed in the ECG from resting conditions.

Our work builds on this by linking the relation between RR and QT intervals to autonomic function and ventricular repolarization dynamics, showing an association between a longer QT-RR adaptation time lag in recovery $\check{\tau}_r$ and SCD in patients with mild to high risk of CAD. Autonomic activity significantly impacts ventricular repolarization in general, and the QT interval in particular, due to the direct autonomic innervation on the ventricular myocardium and as well as of the sinoatrial node activity and its modulation of heart rate [33]. Based on this, the ANS exerts an influence on the QT adaptation to heart rate changes. The study referenced in [34] shows how temporal variations in sympathetic activity have an effect on the QT adaptation time. The study referenced in [35] shows that this phenomenon is discernible in EST stages characterized by increasingly higher sympathetic dominance, where the estimated QT-RR adaptation time becomes successively reducedwhen sympathetic activity is increased. Consequently, the findings of this study suggest a potential association between the observed QT-RR adaptation time lag and the characteristics of ventricular autonomic regulation during EST.

This work is licensed under a Creative Commons Attribution 4.0 License. For more information, see https://creativecommons.org/licenses/by/4.0/

This article has been accepted for publication in IEEE Transactions on Biomedical Engineering. This is the author's version which has not been fully edited and content may change prior to final publication. Citation information: DOI 10.1109/TBME.2025.3607144

Research on QT dynamics early after exercise suggests that impaired autonomic modulation from sympathetic activation to vagal dominance during recovery contributes to arrhythmogenic substrates [34], [36], which is in agreement with our observations. Vuoti et al. [37] found that reduced heart rate variability (HRV) in resting conditions predicts adverse outcomes in CAD patients, supporting the role of RR-based metrics in reflecting autonomic dysfunction. Combining QT-RR adaptation time lag metrics with established markers such as T-wave dispersion and HRV could improve risk stratification. For example, previous studies have shown that combining ECG-based variability measures improves the identification of high-risk individuals [37].

Wong et al. [4] emphasized the global burden of SCD, particularly among CAD patients, and highlighted the need for improved tools to identify high-risk individuals. Our approach provides a complementary perspective to the existing literature by measuring temporal ECG changes during exercise and recovery. The proposed markers may help refine criteria for interventions such as implantable cardioverter defibrillators or targeted medical therapy.

Finally, the results obtained when the QT-RR adaptation time lag in exercise ECG stress testing were computed between the instantaneous $\check{d}^i_{\text{QT}}(n)/\check{d}^i_{\text{RR}}(n)$ and observed $d_{\text{QT}}(n)/d_{\text{RR}}(n)$ series are in line with the findings of our previous study that analyzed another clinical database [23]: elevated values of $\check{\tau}_e$ are indicative of high risk of CAD.

C. Limitations

Although the number of ECGs discarded due to negative estimated time lags was greatly reduced after applying the rule described in Sec.II-C, it would be interesting to investigate different models to fit the data from the exercise and recovery phases of the EST to account for time-varying intra-subject variability and evaluate its impact on the percentage of discarded patients.

The 40-second duration of the selected windows for model identification was chosen as a compromise between the dynamics of the EST protocol (one-minute steps) and data representativeness. Although no significant impact of the selection is expected, a detailed study remains as future work.

Establishing clinical marker thresholds from large clinical studies is essential to confirm the statistical findings and integrate the proposed markers into clinical practice.

Comparing the clinical relevance of the markers presented in this study with other characteristics, or markers, extracted from EST ECGs, such as the area of the QT-RR hysteresis curve, or other methods to estimate the QT-RR adaptation time lag, are an interesting future step to corroborate the relevance of the time lag between the QT and the RR series to predict SCD.

V. Conclusions

The prolongation of QT-RR adaptation time evaluated during the recovery phase of an exercise stress test ECG, calculated as the delay between the observed RR series $d_{\text{RR}}(n)$ and a memoryless RR series, that is, using the RR-based strategy, has been identified as a predictor of SCD and CVD. In contrast, estimating this delay using the $d_{\text{QT}}(n)$ series, that is, the QT-based strategy, results in a marginally significant prediction of CVD and not significant prediction of SCD. These findings, in conjunction with the enhanced robustness to noise demonstrated in simulations for the RR-based strategy, suggest that estimates based on $d_{\text{RR}}(n)$ series are the most reliable to stratification of patients according to their risk of SCD and CVD.

References

[1] N. V. Arteyeva, "Dispersion of ventricular repolarization: Temporal and spatial," *World Journal of Cardiology*, vol. 12, p. 437, 9 2020.

[2] G.-S. Fu, A. Meissner, and R. Simon, "Repolarization dispersion and sudden cardiac death in patients with impaired left ventricular function," *European Heart Journal*, vol. 18, pp. 281–289, 1997.

[3] K. M. Leong, F. S. Ng, C. Roney, C. Cantwell, M. J. Shun-Shin, N. W. Linton, Z. I. Whinnett, D. C. Lefroy, D. W. Davies, S. E. Harding, P. B. Lim, D. Francis, N. S. Peters, A. M. Varnava, and P. Kanagaratnam, "Repolarization abnormalities unmasked with exercise in sudden cardiac death survivors with structurally normal hearts," *Journal of Cardiovascular Electrophysiology*, vol. 29, pp. 115–126, 1 2018.

[4] C. X. Wong, A. Brown, D. H. Lau, S. S. Chugh, C. M. Albert, J. M. Kalman, and P. Sanders, "Epidemiology of sudden cardiac death: global and regional perspectives," *Heart, Lung and Circulation*, vol. 28, no. 1, pp. 6–14, 2019.

[5] K. Zeppenfeld, J. Tfelt-Hansen, M. D. Riva, B. G. Winkel, E. R. Behr, N. A. Blom, P. Charron, D. Corrado, N. Dagres, C. D. Chillou, L. Eckardt, *et al.*, "2022 ESC guidelines for the management of patients with ventricular arrhythmias and the prevention of sudden cardiac death: Developed by the task force for the management of patients with ventricular arrhythmias and the prevention of sudden cardiac death of the european society of cardiology (ESC) endorsed by the association for european paediatric and congenital cardiology (AEPC)," *European Heart Journal*, vol. 43, pp. 3997–4126, 10 2022.

[6] H. Könemann, N. Dagres, J. L. Merino, C. Sticherling, K. Zeppenfeld, J. Tfelt-Hansen, and L. Eckardt, "Spotlight on the 2022 ESC guideline management of ventricular arrhythmias and prevention of sudden cardiac death: 10 novel key aspects," *EP Europace*, vol. 25, pp. 1–12, 5 2023.

[7] Y. Birnbaum, J. M. Wilson, and K. Nikus, "The electrocardiogram in coronary artery disease," pp. 205–216, 2015.

[8] P. Laguna, J. P. M. Cortes, and E. Pueyo, "Techniques for ventricular repolarization instability assessment from the ECG," *Proceedings of the IEEE*, vol. 104, pp. 392–415, 2016.

[9] G. Tse and B. P. Yan, "Traditional and novel electrocardiographic conduction and repolarization markers of sudden cardiac death," *EP Europace*, vol. 19, pp. 712–721, 5 2017.

[10] P. J. Schwartz and S. Wolf, "QT interval prolongation as predictor of sudden death in patients with myocardial infarction." *Circulation*, vol. 57, pp. 1074–1077, 1978.

[11] A. Cabasson, O. Meste, and J. M. Vesin, "Estimation and modeling of QT-interval adaptation to heart rate changes," *IEEE Transactions on Biomedical Engineering*, vol. 59, pp. 956–965, 4 2012.

[12] H. Gravel, D. Curnier, N. Dahdah, and V. Jacquemet, "Categorization and theoretical comparison of quantitative methods for assessing QT/RR hysteresis," p. e12463, 7 2017.

[13] P. Kligfield, K. G. Lax, and P. M. Okin, "QT interval-heart rate relation during exercise in normal men and women: definition by linear regression analysis," *J. Am. Coll. Cardiol.*, vol. 28, no. 6, 1996.

[14] E. Pueyo, P. Smetana, P. Caminal, A. Bayes de Luna, M. Malik, and P. Laguna, "Characterization of QT interval adaptation to RR interval changes and its use as a risk-stratifier of arrhythmic mortality in amiodarone-treated survivors of acute myocardial infarction," *IEEE Trans. Biomed. Eng.*, vol. 51, no. 9, 2004.

[15] P. Smetana, E. Pueyo, K. Hnatkova, V. Batchvarov, P. Laguna, and M. Malik, "Individual patterns of dynamic QT/RR relationship in survivors of acute myocardial infarction and their relationship to antiarrhythmic efficacy of amiodarone," *Journal of Cardiovascular Electrophysiology*, vol. 15, pp. 1147–1154, 10 2004.

This work is licensed under a Creative Commons Attribution 4.0 License. For more information, see https://creativecommons.org/licenses/by/4.0/

This article has been accepted for publication in IEEE Transactions on Biomedical Engineering. This is the author's version which has not been fully edited and content may change prior to final publication. Citation information: DOI 10.1109/TBME.2025.3607144

[16] A. Grom, T. S. Faber, M. Brunner, C. Bode, and M. Zehender, "Delayed adaptation of ventricular repolarization after sudden changes in heart rate due to conversion of atrial fibrillation. a potential risk factor for proarrhythmia?" *Europace*, vol. 7, pp. 113–121, 1 2005.

[17] A. Martín-Yebra, L. Sörnmo, and P. Laguna, "QT interval adaptation to heart rate changes in atrial fibrillation as a predictor of sudden cardiac death," *IEEE Trans. Biomed. Eng.*, vol. 69, no. 10, pp. 3109–3118, 2022.

[18] P. D. Arini, G. C. Bertrán, E. R. Valverde, and P. Laguna, "T-wave width as an index for quantification of ventricular repolarization dispersion: Evaluation in an isolated rabbit heart model," *Biomedical Signal Processing and Control*, vol. 3, pp. 67–77, 1 2008.

[19] A. Mincholé', A. Bueno-Orovio, P. Laguna, E. Pueyo, and B. Rodríguez, "ECG-based estimation of dispersion of APD restitution as a tool to stratify sotalol-induced arrhythmic risk," *Journal of Electrocardiology*, vol. 48, pp. 867–873, 9 2015.

[20] J. Ramírez, M. Orini, A. Mincholé', V. Monasterio, I. Cygankiewicz, A. B. de Luna, J. P. Martínez, P. Laguna, and E. Pueyo, "Sudden cardiac death and pump failure death prediction in chronic heart failure by combining ecg and clinical markers in an integrated risk model," *PLoS ONE*, vol. 12, 10 2017.

[21] J. Ramírez, A. Kiviniemi, S. van Duijvenboden, A. Tinker, P. D. Lambiase, J. Junttila, J. S. Perkiömäki, H. V. Huikuri, M. Orini, and P. B. Munroe, "ECG T-wave morphologic variations predict ventricular arrhythmic risk in low- and moderate-risk populations," *Journal of the American Heart Association*, vol. 11, p. e025897, 2022.

[22] K. D. Rizas, T. Nieminen, P. Barthel, C. S. Zürn, M. Kähönen, J. Viik, T. Lehtimäki, K. Nikus, C. Eick, T. O. Greiner, H. P. Wendel, P. Seizer, J. Schreieck, M. Gawaz, G. Schmidt, and A. Bauer, "Sympathetic activity-associated periodic repolarization dynamics predict mortality following myocardial infarction," *J. Clin. Investig.*, vol. 124, 2014.

[23] C. Pérez, E. Pueyo, J. P. Martínez, J. Viik, and P. Laguna, "QT interval time lag in response to heart rate changes during stress test for coronary artery disease diagnosis," *Biomed. Signal Process. Control*, vol. 86, p. 105056, 2023.

[24] C. Pérez, E. Pueyo, J. P. Martínez, J. Viik, L. Sörnmo, and P. Laguna, "Performance evaluation of QT-RR adaptation time lag estimation in exercise stress testing," *IEEE Transactions on Biomedical Engineering*, 2024.

[25] M. J. Junttila, A. M. Kiviniemi, E. S. Lepojärvi, M. Tulppo, O. P. Piira, T. Kenttä, J. S. Perkiömäki, O. H. Ukkola, R. J. Myerburg, and H. V. Huikuri, "Type 2 diabetes and coronary artery disease: Preserved ejection fraction and sudden cardiac death," *Heart Rhythm*, vol. 15, pp. 1450–1456, 2018.

[26] P. W. Serruys, M.-C. Morice, A. P. Kappetein, A. Colombo, D. R. Holmes, M. J. Mack, E. Stahle, T. E. Feldman, M. van den Brand, E. J. Bass, N. V. Dyck, K. Leadley, K. D. Dawkins, and F. W. Mohr, "Percutaneous coronary intervention versus coronary-artery bypass grafting for severe coronary artery disease," *New England Journal of Medicine*, vol. 360, pp. 961–972, 3 2009.

[27] E. Pueyo, M. Malik, and P. Laguna, "A dynamic model to characterize beat-to-beat adaptation of repolarization to heart rate changes," *Biomed. Signal Process. Control*, vol. 3, no. 1, pp. 29–43, 2008.

[28] S. Romagnoli, A. Sbrollini, L. Burattini, J. P. Martínez, and P. Laguna, "Characterization of QT-interval adaptation time lag in response to sport-induced heart rate changes measured from wearable ECG recording," *IEEE Trans. Biomed. Eng.*, vol. 71, no. XX, pp. xx–xx, 2025.

[29] S. Romagnoli, C. Peréz, L. Burattini, E. Pueyo, M. Morettini, A. Sbrollini, J. P. Martínez, and P. Laguna, "Model-based estimators of QT series time delay in following Heart-Rate changes," *45th Ann. Int. Conf. IEEE Eng. Med. Biol. Soc. (EMBC)*, pp. 1–4, 2023.

[30] L. S. Fridericia, "Die systolendauer im elektrokardiogramm bei normalen menschen und bei herzkranken," *Acta Medica Scandinavica*, vol. 53, no. 1, pp. 469–486, 1920.

[31] J. J. Hekkanen, T. V. Kenttä, M. A. E. Haukilahti, J. T. Rahola, L. Holmström, J. Vähätalo, M. P. Tulppo, A. M. Kiviniemi, L. Pakanen, O. H. Ukkola *et al.*, "Increased beat-to-beat variability of T-wave heterogeneity measured from standard 12-lead electrocardiogram is associated with sudden cardiac death: a case–control study," *Frontiers in Physiology*, vol. 11, p. 1045, 2020.

[32] J. T. Rahola, S. M. Mattila, A. M. Kiviniemi, O. H. Ukkola, M. P. Tulppo, M. J. Junttila, H. V. Huikuri, T. V. Kenttä, and J. S. Perkiömäki, "Prognostic significance of beat-to-beat variability of spatial heterogeneity of repolarization analyzed from a 5-minute resting electrocardiogram in coronary artery disease," *Heart Rhythm*, 2024.

[33] S. Nayyar, K. C. Roberts-Thomson, M. A. Hasan, T. Sullivan, J. Harrington, P. Sanders, and M. Baumert, "Autonomic modulation of repolarization instability in patients with heart failure prone to ventricular tachycardia," *American Journal of Physiology - Heart and Circulatory Physiology*, vol. 305, pp. 1181–1188, 10 2013.

[34] D. A. Sampedro-Puente, J. Fernández-Bes, N. Szentandrássy, P. Nánási, P. Taggart, and E. Pueyo, "Time course of low-frequency oscillatory behavior in human ventricular repolarization following enhanced sympathetic activity and relation to arrhythmogenesis," *Frontiers in Physiology*, vol. 10, 1 2020.

[35] C. Pérez, R. Cebollada, K. A. Mountris, J. P. Martínez, P. Laguna, and E. Pueyo, "The role of β-adrenergic stimulation in qt interval adaptation to heart rate during stress test," *Plos One*, vol. 1, 1 2023.

[36] E. Pueyo, A. Corrias, L. Virág, N. Jost, T. Szél, A. Varró, N. Szentandrássy, P. P. Nánási, K. Burrage, and B. Rodríguez, "A multiscale investigation of repolarization variability and its role in cardiac arrhythmogenesis," *Biophysical journal*, vol. 101, no. 12, pp. 2892–2902, 2011.

[37] A. O. Vuoti, M. P. Tulppo, O. H. Ukkola, M. J. Junttila, H. V. Huikuri, A. M. Kiviniemi, and J. S. Perkiömäki, "Prognostic value of heart rate variability in patients with coronary artery disease in the current treatment era," *PloS one*, vol. 16, no. 7, p. e0254107, 2021.

This work is licensed under a Creative Commons Attribution 4.0 License. For more information, see https://creativecommons.org/licenses/by/4.0/

This article has been accepted for publication in IEEE Transactions on Biomedical Engineering. This is the author's version which has not been fully edited and content may change prior to final publication. Citation information: DOI 10.1109/TBME.2025.3607144

Supplementary Material

LIST OF ACRONYMS

This list provides definitions of specific acronyms used in this article.

- SCD: Sudden Cardiac Death
- CAD: Coronary Artery Disease
- ICD: Implantable Cardioverter Defibrillator
- CVD: Cardiovascular Death
- $d_{\text{RR}}(n)$: observed RR series.
- $d_{\text{QT}}(n)$: observed QT series.
- $d^i_{\text{RR}}(n)$: memoryless RR series related to the observed QT series through a memoryless transformation, using information from the concatenated windows $W_b \cup W_e \cup W_{lr}$ to compute the model parameters α and β.
- $d^i_{\text{QT}}(n)$: instantaneous QT series related to the observed RR series through a memoryless transformation, using information from the concatenated windows $W_b \cup W_e \cup W_{lr}$ to compute the model parameters α and β.
- $\check{d}^i_{\text{RR}}(n)$: memoryless RR series related to the observed QT series through a memoryless transformation, after modifying [QT, RR] data pairs of window W_e.
- $\check{d}^i_{\text{QT}}(n)$: instantaneous QT series related to the observed RR series through a memoryless transformation, after modifying [QT, RR] data pairs of window W_e.
- EST: exercise stress test.
- $\mathcal{HZR}$: hazard ratio.
- SXscore: SYNTAX score.
- SXscore-LR: low-risk group with a SXscore lower than 23.
- SXscore-MR: mild-risk group with a SXscore between 23 and 33.
- SXscore-HR: high-risk group with a SXscore higher than 33.
- W_b: learning window taken in the baseline rest phase before the EST started.
- W_e: learning window centered on the peak exercise.
- W_{lr}: learning window taken at the end of the EST, which corresponds to a rest area at the late recovery phase.
- $\check{\tau}_e$: QT-RR adaptation time lag estimate during the exercise phase of EST, after modifying [QT, RR] data pairs from window W_e.
- $\check{\tau}_r$: QT-RR adaptation time lag estimate during the recovery phase of EST, after modifying [QT, RR] data pairs from window W_e.
- $\Delta_{\check{\tau}}$: Difference between $\check{\tau}_r$ and $\check{\tau}_e$.
- $\hat{\tau}_e$: initial estimate of QT-RR adaptation time lag during the exercise phase of EST necessary to modify data pairs from W_e.
- ϵ_τ: error between the estimated QT-RR adaptation time lag and the true time lag between the RR and QT series using simulated EST ECGs.

This work is licensed under a Creative Commons Attribution 4.0 License. For more information, see https://creativecommons.org/licenses/by/4.0/